Biochemistry and Biophysics Reports 28 (2021) 101155

Contents lists available at ScienceDirect

Biochemistry and Biophysics Reports

journal homepage: www.elsevier.com/locate/bbrep

Role of aspartic acid residues D87 and D89 in APS kinase domain of human 3′-phosphoadenosine 5′-phosphosulfate synthase 1 and 2b: A commonality with phosphatases/kinases

K.V. Venkatachalam [a,*], Rudiger H. Ettrich [b,c]

[a] College of Allopathic Medicine, Nova Southeastern University, Ft. Lauderdale, FL, 33328, USA
[b] College of Biomedical Sciences, Larkin University, Miami, FL, 33169, USA
[c] Faculty of Mathematics and Physics, Charles University, 121 16, Prague, Czech Republic

ARTICLE INFO

Keywords:
Enzyme mechanism
Enzyme catalysis
Enzyme structure
Phosphoryl transfer
Phosphorylation

ABSTRACT

3′-phosphoadenosine 5′-phosphosulfate (PAPS) is synthesized in two steps by PAPS synthase (PAPSS). PAPSS is comprised of ATP sulfurylase (ATPS) and APS kinase (APSK) domain activities. ATPS combines inorganic sulfate with α-phosphoryl of ATP to form adenosine 5′-phosphosulfate (APS) and PPi. In the second step APS is phosphorylated at 3′-OH using another mole of ATP to form PAPS and ADP catalyzed by APSK. The transfer of gamma-phosphoryl from ATP onto 3′-OH requires Mg_2^+ and purported to involve residues $D_{87}GD_{89}N$. We report that mutation of either aspartic residue to alanine completely abolishes APSK activity in PAPS formation. PAPSS is an, unique enzyme that binds to four different nucleotides: ATP and APS on both ATPS and APSK domains and ADP and PAPS exclusively on the APSK domain. The thermodynamic binding and the catalytic interplay must be very tightly controlled to form the end-product PAPS in the forward direction. Though APS binds to ATPS and APSK, in ATPS domain, the APS is a product and for APSK it is a substrate. DGDN motif is absent in ATPS and present in APSK. Mutation of D_{87} and D_{89} did not hamper ATPS activity however abolished APSK activity severely. Thus, $D_{87}GD_{89}N$ region is required for stabilization of Mg^{2+}-ATP, in the process of splitting the γ-phosphoryl from ATP and transfer of γ-phosphoryl onto 3′-OH of APS to form PAPS a process that cannot be achieved by ATPS domain. In addition, gamma^{32}P-ATP, trapped phosphoryl enzyme intermediate more with PAPSS2 than with PAPSS1. This suggests inherent active site residues could control novel catalytic differences. Molecular docking studies of hPAPSS1with ATP + Mg^{2+} and APS of wild type and mutants supports the experimental results.

1. Introduction

3′-Phosphoadenosine 5′-Phosphosulfate (PAPS) is the universal sulfuryl donor synthesized by PAPS Synthase (PAPSS) in two steps [1]. First inorganic sulfate oxyanion reacts with α-phosphoryl of ATP to form APS and PPi catalyzed by ATP sulfurylase (ATPS) domain activity of PAPSS. In the second step APS is phosphorylated at the 3′-OH of APS using ATP by APSK domain activity of PAPSS to form PAPS and ADP [2] (Fig. 1). Being an α−β phosphorolytic reaction, ATPS uses the motif HNGH where the two histidine's are essential for catalytic activity. Mutation of the two histidine's (H_{425} and H_{428}) in PAPSS to alanine completely abolishes the α−β bond cleavage activity of ATPS in forming APS and PPi [3]. Half reaction of this histidine to alanine mutant enzyme retained complete APSK activity. Thus, the domain activities are separate, and site selected mutation of each domain doesn't perturb the non-mutated domain activity. In APSK reaction, ATP is cleaved between β−γ phosphates and the binding of ATP involves classical Walker A motif (G-x (4)-GK-[T/S]), also called P loop for phosphate binding. P loop walker A or B motifs are present in many ATP binding and ATP β−γ splitting enzymes [4–7]. A synthetic peptide that binds to the P-loop has been described [8]. In murine PAPSS the P-loop motif of ($G_{59}LSG_{62}AG_{64}K_{65}T$) is present [9]. Mutation of the G_{64} and K_{65} residues to alanine abolishes the APSK activity [9]. In APSK once the binding is established, the γ-phosphoryl of ATP is transferred to 3′-OH of the APS to form PAPS. Unlike many kinases that possess P-loop to bind single nucleotide ATP in the binding pocket, APSK had to accommodate two nucleotides, a sulfo-phospho nucleotide

* Corresponding author.
E-mail address: venk@nova.edu (K.V. Venkatachalam).

https://doi.org/10.1016/j.bbrep.2021.101155
Received 25 June 2021; Received in revised form 6 October 2021; Accepted 15 October 2021

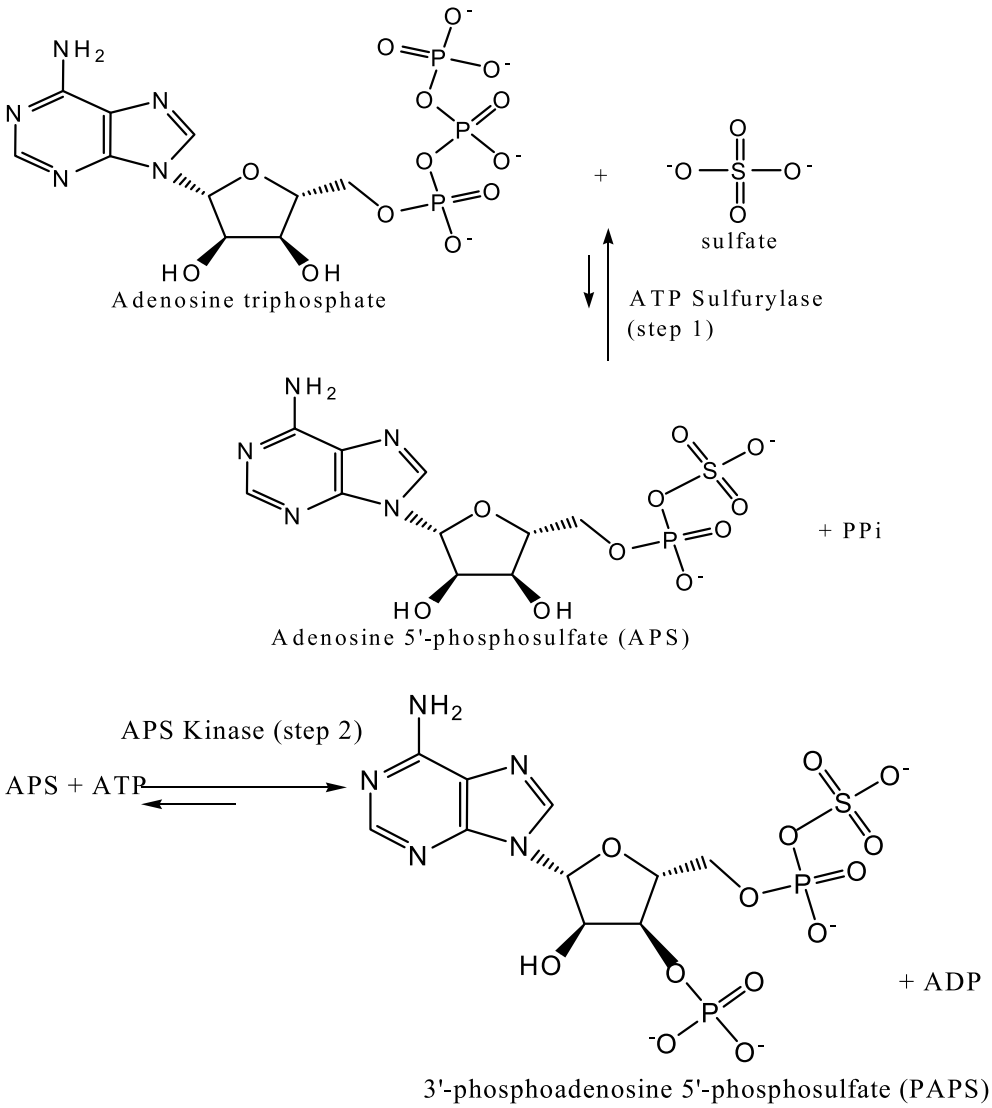

Fig. 1. Sequential Synthesis of 3′-phosphoadenosine 5′-phosphosulfate (PAPS) from inorganic sulfate (SO_4^{2-}) and 2 mol of ATP by the bifunctional enzyme 3′-phosphoadenosine 5′-phosphosulfate synthase (PAPSS). In the first step the sulfuryl oxyanion is purported to react with α-phosphoryl of ATP to form 3′-phosphoadenosine 5′-phosphosulfate (APS) by the ATP sulfurylase (ATPS) domain activity. In the second step APS reacts with another molecule of ATP. In this step the 3′-oxyanion is purported to react with γ-phosphoryl of the ATP to form the final product PAPS and ADP catalyzed by the APS kinase domain activity of the PAPSS. The full reaction of PAPS formation is depicted below.

(APS) and a phospho nucleotide (ATP). APSK like *E. coli* 3′-nucleotidase and phosphotransferase/phosphatase motif of (DXDX (T/V) [10,11], possess conserved DXDX residues. In PEP carboxykinase there are conserved aspartic acid residues that are reported to interact with metal ions Mg_2^+ and Mn_2^+ that are required for phosphorylation reaction [12]. These aspartic acid residues are 23–24 residues downstream from the start residue glycine of the Walker A motif. In APSK domain of the bifunctional human PAPSS1(hPAPSS1) the two purported aspartic acid residues are about 27–29 residues downstream to the first glycine residue of the Walker A motif (GLSGAGK) [2]. Interestingly in hPAPSS2a the two crucial aspartic acid residues are 23–24 residues downstream to the Walker A motif like that of PEPCK. In hPAPSS2b isoform/isozyme, the spacing between Walker A motif and aspartic acid residues are like that of hPAPSS1. Catalytic efficiencies of hPAPSS1, 2a and 2b in overall PAPS formation are quite different [13,14]. In this report the mutation of the two aspartic acid residues of hPAPSS1 and its consequence on the APSK activity is presented. Mutation of D_{87} and D_{89} into alanine completely abolished APSK activity without altering the ATPS activity. Computational studies using molecular docking supports the notion that the aspartic acid residues are required for stabilizing the phosphate bound Mg^{2+} to neutralize the positive charges of the metal cation. Incubation of hPAPSS1 and hPAPSS2b with ^{32}Pγ-ATP transferred labeled γ-phosphoryl on to hPAPSS2b and hPAPSS1 supporting the transient role of one of the aspartic residues in phosphorolysis on the overall catalysis. The covalent phosphoryl intermediate trapped was more with PAPSS2 compared to PAPSS1 suggesting inherent catalytic differences between isoforms. Molecular docking studies with ATP + Mg^{2+} and APS of wild type and mutants were performed that supports the experimental results and allow atomistic interpretation of the proposed mechanism.

2. Materials and methods

Materials: Radionucleotides [α-^{35}S]ATP for DNA sequencing, inorganic [^{35}S]SO_4 (1300 Ci/mmol), and [^{35}S]PAPS for enzyme assays were purchased from NEN Life Science Products. Oligonucleotides were obtained from Life Technologies, Inc. and Gene Probe Technology (Gaithersburg, MD). Site-directed mutagenesis kit was obtained from Stratagene (La Jolla, CA). Version-2 sequencing kit was obtained from U. S. Biochemical Corp. Agarose was purchased from FMC BioProducts (Rockland, ME) and polyethyleneimine cellulose (PEI)-TLC plates were purchased from Merck.

Overexpression of Human PAPS Synthase and Mutant Constructs-Wild type full-length hPAPS synthase (GenBankTM accession number U53447) and mutant hPAPS synthase constructs were amplified by PCR using primers designed to contain *Bam*HI restriction sites, cloned into *Bam*HI digested pET-19b vectors containing a proprietary 122 base pair *Nco*I-*Nde*I cassette (Veritas, Potomac, MD) encoding the calmodulin-binding site of calcineurin followed by a histidine tag and an enter

okinase cleavage site, and used for transformation of *Escherichia coli* essentially as described previously [2]. Plasmids were used for transformation of DH-5α competent *E. coli* cells by the $CaCl_2$ method. Transformants were isolated and miniprepped, and plasmids were sequenced for correct orientation of the initiator codon with respect to the T7 promoter sequence. The pET-19b vectors containing the correct inserts were isolated and used for transformation of expression host cells from Stratagene (BL21-DE3 plyz).

Site-selected Mutagenesis—The conserved purported phosphotransferase motif (DxDx (T/V)) located in the NH_2-terminal region of human PAPS synthase was subjected to mutational analysis. Thus, amino acid substitutions were carried out in the T**LDGD** sequence (amino acids 85–89). Site-selected mutagenesis was performed according to Stratagene's quik change mutagenesis kit. For example, oligonucleotides containing the respective base substitutions were synthesized. Employing the wild type hPAPS synthase expression vector plasmid pET-19b, mutations were performed by PCR using the substituted primer and Pfu DNA polymerase. Thermal cycle phases consisted of either 12 cycles of denaturation at 94 °C for 30 s, annealing at 55 °C for 1 min, and extension at 68 °C for 12 min. After PCR, the methylated parent template plasmid was digested with the *Dpn*I restriction enzyme, and the circular dsDNA was used to transform XL1-Blue supercompetent cells. Colonies were isolated, miniprepped, and sequenced. Verified mutant plasmids were used to transform pLyz BL21-DE3 overexpression bacteria that are deficient in proteases. Plasmids were isolated and sequenced to verify the presence of the proper mutation. Preparation of Bacterial Cell Extracts—Colonies were grown in LB broth containing ampicillin to an A595 nm of 0.5, and IPTG was added to a final concentration of 1 mM to induce expression. Induction was carried out for 3 h. Cells were collected by centrifugation, the pellets were resuspended in 150 ml of lysis buffer (20 mM Tris-HCl, pH 7.5, containing 50 mM KCl, 1 mM dithiothreitol, 10% glycerol, and 1.2 mg/ml lysozyme), and the cell suspension was transferred to a microcentrifuge tube. The original tube was washed with 100 ml of lysis buffer, the wash was added to the cell suspension, cell lysis was carried out by incubation at 25 °C for 7 min, and lysates were centrifuged for 15 min at 10,000 g at 4 °C.

PAPS Synthase Assay—Enzyme activity was determined in a total volume of 10 μl consisting of 3 μl of sample, 3 μl of reaction buffer (150 mM Tris-HCl, pH 8.0, 50 mM KCl, 15 mM $MgCl_2$, 3 mM EDTA, and 45 mM dithiothreitol), 1 μl of 50 mM ATP, and 3 μl of inorganic [^{35}S]SO_4 (~3.4 μCi). Reactions were carried out for 30 min at 37 °C and stopped by placing the reaction tubes in boiling water for 5 min. Aliquots (1 μl) were transferred to PEI-TLC plates and developed using 0.9 M LiCl as the solvent system. Following chromatography, the PEI-TLC plates were dried and exposed overnight to x-ray film (Eastman Kodak Co.). The respective spots for PAPS, APS, and SO_4 were excised, and the radioactivity was determined by liquid scintillation.

2.1. Binding and/or phosphotransfer of γP^{32}-ATP onto wildtype hPAPSS1, hPAPSS2b, and mutants D_{87} D_{89}

Bacteria expressed proteins from wildtype hPAPSS1, hPAPSS2b, and Mutants D_{87} D_{89} were purified according to the procedures published earlier. In brief the bacterial lysates from the respective clones were filtered through cheese cloth and the filtrate was mixed with N-NTA (Qiagen Inc.,) slurry and it was gently mixed at 100 rpm on a rotatory shaker for 90 min. The slurry was then packed on to a column and washed with (50 mM Tris-HCl pH 8.0, 30 mM NaCl, 1 mM β-mercaptoethanol and protease inhibitor cocktail (Calbiochem) and 20 mM imidazole) containing buffer until no proteins could be detected. The column was then eluted with buffer which is same as wash buffer except it contained 250 mM imidazole. 12 μL of purified proteins (~0.1 μg) were incubated in reaction buffer (150 mM Tris-HCl, pH 8.0, 50 mM KCl, 15 mM $MgCl_2$, 3 mM EDTA, and 45 mM dithiothreitol) containing 1 μL (10 μCi) of ATP (5000 Ci/nMol) in a total volume of 25 μL. The reaction was incubated at 4 °C for 10 min and then stopped with SDS-PAGE sample buffer (50 mM Tris-HCl pH 6.8, 2.5% SDS, 12% sucrose, 2 mM DTT, 0.02% brilliant blue) and boiled for 5 min. The samples were briefly spun and ~38 μL was loaded on to 10% SDS-PAGE gels (Novex) and electrophoresed. The gel was then dried and exposed to X-ray film overnight.

Amino Acid Sequence Alignment Analyses-Searches of the protein sequence data base (the nonredundant data base at the NCBI) were performed using the gapped BLAST program, the position-specific iterative BLAST (PSI-BLAST), and the pattern-hit initiated BLAST (PHI-BLAST) programs. Multiple alignments were constructed using either the Clustal W program or the MACAW program.

Preparation of APS-Kinase domain of human PAPSS1 for molecular docking-All molecular modelling was performed using YASARA Structure version 20.12.24 [15,16]. The 1.9 Å resolution crystal of the active conformation of the APS-Kinase domain of human PAPSS1 in complex with ADPMg and PAPS was retrieved from the Protein Data Bank (PDBID:2OFX; [17]). The three-dimensional structure contains two identical chains, A and B. The full structure was used for all docking experiments, with both chains being present. However, chain B was chosen for placing the simulation cell and as receptor site for docking. All ligands, phosphate and water molecules were removed, and hydrogen atoms were added using the standard procedure in Yasara including energy minimization performed on the entire structure. Mg-ATP and APS were prepared starting from available ligand structures in the Protein Data Bank and using the automatic force field parameter assignment in YASARA, AutoSMILES. AutoSMILES employs SMILES strings to identify known molecules and resorts to the AM1BCC [18] and GAFF [19] (General AMBER force field) approaches for all other molecules. AM1BCC charges are additionally improved by using known RESP charges of similar molecule fragments and calculation of semi-empirical AM1 Mulliken point charges [20]. This step involves a geometry optimization with the COSMO solvation model [21].

Molecular Docking-Molecular docking experiments were prepared using YASARA [15,16]. Yasara implements AutoDock-Vina [22] which uses iterated local search global optimizer algorithm for prediction binding poses and semiempirical scoring function for evaluation and ranking of binding.

To allow the program to identify and find the binding pockets in an unbiased way as search space larger than domain B was used by defining a simulation cell at least 5 Å around all atoms of this domain. 100 Docking runs in the global search mode of AutoDock VINA [22] implemented in YASARA [15] were calculated for docking the ligands to the APS-Kinase domain of human PAPSS1. The runs then were clustered into distinct complex conformations that all differ by at least 5.0 Å heavy atom RMSD, and the pose with the best binding energy in each cluster was taken as representing this conformation. During docking the protein was kept rigid while the ligand was fully flexible. Firstly, we performed re-docking of PAPS and ADP (including the magnesium ion) to be sure the program correctly identifies the binding sites as seen in the crystal structure for both ligands. In all cases APS has been docked first and MgATP second. The pose with the highest binding energy was taken as the representative structure for this cluster. Single point mutations D89A, D87A and T85A were introduced in each monomer of APSK domain of human PAPSS1in Yasara, always followed by energy minimization using the Amber 03 force field to match the forcefield used for docking. Figures were created in Yasara and rendered using POVRay (www.povray.org). Final editing and labeling were done in GIMP 2.10.18 (www.gimp.org).

3. Results

3.1. Amino acid sequence analysis

Amino acid sequence analysis of bifunctional fused gene products of PAPSS were compared and analyzed. For PAPSS the N-terminal region spanning up to ~219 amino acids are comprised of key residues/motif's

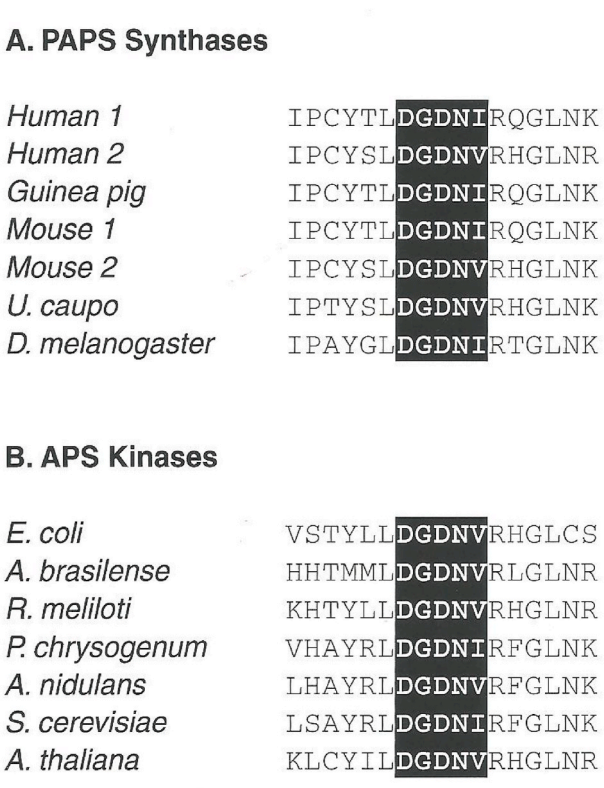

Fig. 2. Comparison of amino acid sequence of APS kinase in fused gene products of PAPSS and individual APS kinase of various organisms. In Fig. 2a, PAPSS partial amino acid sequence from several different organisms, within organism, and the isoforms 1 and 2 are compared. Genbank accession numbers are in parentheses. human (*homo sapiens*) PAPSS (hPAPSS1, AAC39894), (hPAPSS2b, AAF20366); guinea pig (*Cavia Porcellus*) (AAC02266); mouse (*Mus musculus*) (mPAPSS1, AAH66055), (mPAPSS1b/transcript variant 2, NP_001276406); worm (*Urechis caupo*), (uPAPSS, Q27128); fly (*Drosophila melanogaster*), (dPAPSS, CAA73368). Fig. 2b depicts the comparison of APS kinase individual polypeptide sequence comparison from various organisms. The cys N gene product of *E. coli* (M74586); nod Q gene products of the symbiotic bacteria *Azospillium brasilense, (A. brasilense)* (M94886); *Rhizobium meliloti (R. meliloti)* (M68858); *Penicillium chrysogenum (P. chrysogenum)*, (U07353); *Aspergillus nidulans, (A. nidulans)* (×82541); the plant *Arabidopsis thaliana, (A. thaliana)* (U05218); yeast *Saccharomyces cerevisiae (s. cerevisiae)* (08536).

required for binding of phospho and sulfo nucleotides essential for forward and backward reactions of APS kinase domain. For the catalytic activities of hPAPSS1 the linker region (L_{220}QERDIVPVDASYEVKELYVPENKLHLAKTDAETLPALKINKVDMQ$_{265}$) is perhaps required for completing the reaction and release of products (Venkatachalam et al., unpublished). For sequence comparison PAPSS1 and PAPSS2 from human and mouse were used. In addition, guinea pig, worm (*Urechis caupo*), fly (*Drosophila melanogaster*) sequences were analyzed. All the compared PAPSS full length sequences contained DGDN conserved aspartic acid residues (Fig. 2A). In addition, DGDN residues were analyzed for its presence in *Escherichia coli, Azospirillum brasilense, Rhizobium meliloti, Penicillium chrysogenum, Aspergillus nidulans, Saccharomyces cerevisiae and Arabidopsis thaliana* in which APSK is an unfused single gene product (Fig. 2B). In other words, the organisms analyzed in Fig. 2B possess APSK as a separate enzyme independent of ATPS and are coded by separate genes. For example, in *E. coli* (Cys C) codes for APSK and Cys D, N, codes for ATPS. All of the organisms compared in Fig. 2B, possessed the residues (DGDN) involved for putative 3′-OH phosphorylation on the independent APSK enzyme or the activity domain of fused PAPSSS compared in Fig. 2A.

3.2. Mutation of DxDx motif in hPAPSS1

Though APS binding is part of the ATPS backward reaction the motif DGDN is absent which clearly support the notion that DGDN residues are unique to APSK domain for PAPS formation. In all 3 mutants and wild type ATPS activity was not affected (3A). Mutation of the D_{87}, D_{89} residues to alanine completely abolished the APSK activity in forming PAPS (Fig. 3B, Table 1A). This clearly supports the notion that the phosphorylation of 3'-OH of APS involves D_{87}, D_{89} residues. Mutation of the T_{85} to Alanine did not decrease the PAPS formation (Fig. 3B, Table 1B). Wildtype, T_{85}A, D_{87}A and D_{89}A were all assayed for overall formation of PAPS. Wildtype PAPS formation was taken as 100% activity and T_{85}A mutant had slightly higher PAPS formation, a gain of function. It is interesting that in D_{87}A and D_{89}A mutants, the ATPS activity was unaffected and the overall formation of APS, ~equal to that of APS + PAPS formed in wild type (Fig. 3C).

3.3. Binding/phosphotransfer of γP^{32}-ATP onto wildtype hPAPSS1, hPAPSS2b, and mutants D_{87} D_{89}

Bacteria expressed proteins from wildtype hPAPSS1, hPAPSS2b, and Mutants D_{87} and D_{89} were purified according to the procedures published earlier. In brief, the bacterial lysates from the respective clones were purified. Purified proteins were allowed to bind/react with γP^{32}-ATP and the respective proteins electrophoresed on SDS-PAGE and autoradiographed. Both D_{87} and D_{89} did not show any band corresponding to PAPSS (~70 kDa) like mock controls that lacked PAPSS. Whereas wildtype hPAPSS1 (weak) and hPAPSS2b (strong) radioactive band revealed by autoradiography (Fig. 4).

3.4. Molecular modelling

Molecular docking studies show the 3′-OH within 1.8 Å to the carboxyl of D89 (Fig. 5, panel D) and indicate that the metal ion Mg^{2+} could easily move into to proximity of the ribosyl hydroxyl that in essence facilitates 3′-phosphorylation of the sulfonucleotide APS (Fig. 5, panel D). Similar analysis of an ATPS crystal structure from available PDB data (PDBID: 1ZUN) didn't show the effect of metal ion interactive part at 3′-OH of APS. This clearly confirms that the two domains ATPS and APSK functions independently. ATPS in the forward direction binds ATP and sulfate to form the products APS and PPi. Though the ATP binding part is common between APSK and ATPS in ATPS active site, the ATP is split between the a-b phosphoanhydride bond that neither has the typical DGDN type motif for Mg^{2+} chelation nor has the typical Walker A motif. Being an alpha-beta splitting enzyme, it has the proven HNGH motif and downstream to that, it has aspartic residues at position 9, 34,35 and 36 in an undefined manner unlike clear DGDN motif present in APSK. The roles of quasi aspartic acid residues downstream (434, 459, 460, 461) to HNGH motif in ATPS if any needs to be assigned. This could explain that ATP-Mg^{2+} chelation decides the thermodynamic favorability of ATP splitting. ATPS reaction in the forward reaction is unfavorable partly due to poor Mg^{2+} chelation and relatively stable alpha-beta bond compared to APSK active site where the ATP is more facile. The sulfuryl of sulfate and APS are stabilized by positively charged arginine residues without chelation of cation such as Mg^{2+} (Venkatachalam, Ettrich unpublished).

4. Discussion

The absence of the linker region between ATPS domain and APSK results in nonfunctional enzyme [1]. In hPAPSS1 the C-terminus that possess ATPS activity spans from 220 to 623, wherein the residues corresponding to 220–265 encompasses linker region (Fig. 6). Residues 266–623 must be required for the phospho (ATP and AMP) and sulfo (APS) nucleotide binding that are required for forward and reverse reactions of ATPS. ATPS being a α−β ATP splitting enzyme uses

A

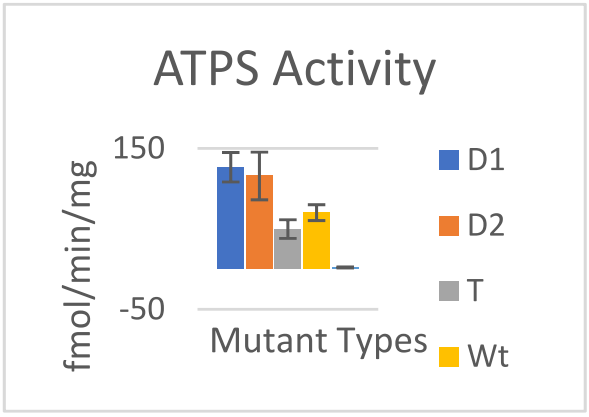

B

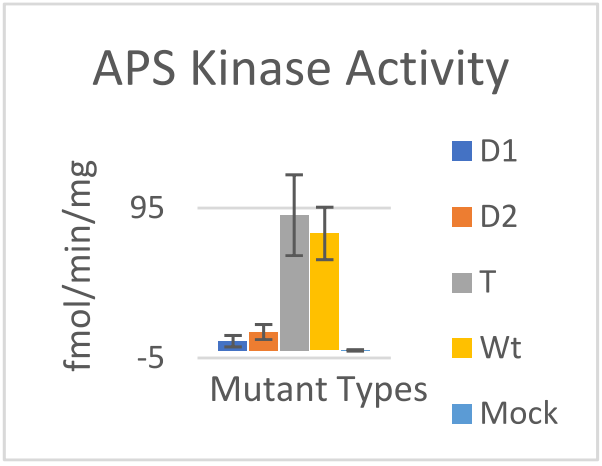

C

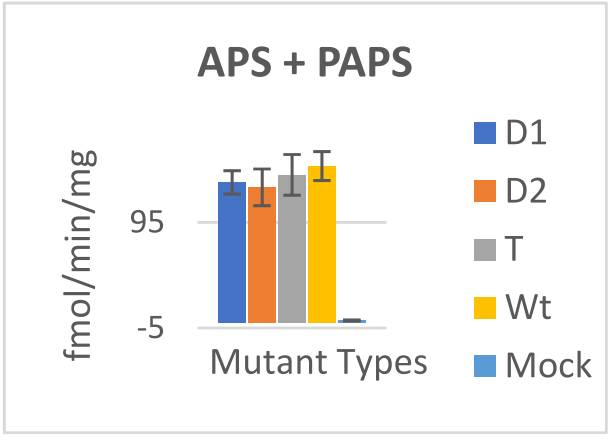

(caption on next column)

Fig. 3. PAPS Synthase Assay-Enzyme activity was determined for wildtype (WT), various mutants T85A, D87A, D89A, and mock control using $^{35}SO_4$ labeled substrate and ATP in a total volume of 10 μl as described in detail in the method section. Reactions were carried out for 30 min at 37 °C and stopped by placing the reaction tubes in boiling water for 5 min. Aliquots (1 μl) were transferred to PEI-TLC plates and products separated. Following chromatography, the PEI-TLC plates were dried and exposed overnight to x-ray film (Eastman Kodak Co.). The respective spots for PAPS (the final product), APS (intermediate), and SO_4 (substrate) were excised, and the radioactivity was determined by liquid scintillation. Values were converted into specific activities (fmol/min/mg) and plotted. In panel A the intermediate APS formed is shown. In panel B the final product PAPS (the product of ATP sulfurylase + APS kinase) is shown. As compared between panel A and B, both the mutants D87A and D89A retained full activity of ATP sulfurylase and lacked complete activity of APS kinase as shown by only formation of APS. The nearby residue mutant T85A, was nearly same as wildtype and it exhibited both ATP sulfurylase and APS kinase activity as shown by the respective formation of APS and PAPS equivalent to wild type (WT). It is interesting that the sum of (intermediate (APS) + product (PAPS)) of WT, T85A, D87A and D89A were equal, confirming that the mutations did not perturb ATPS (Panel C).

$H_{425}NGH_{428}$ motif for ATP binding similar, to type I tRNA synthetases [2]. Mutation of the two crucial histidine residues ($H_{425,}$ H_{428}) completely abolished the ATPS activity in the forward and backward directions.

Though both domains bind APS, (ATPS for backward reaction) and (APSK for forward reaction), the phosphorylation of APS to form PAPS happens only in APSK. Once PAPS is formed it must leave the activesite followed by ADP, facilitating the entry of new ATP and APS for another round of catalysis. Since ATP is the common substrate for both ATPS and APSK it would bind independently onto the respective site in ATPS waiting for sulfate to react with to form APS and in APSK waiting for APS to be released from ATPS to bind with APSK. From unpublished report (Venkatachalam et al.), found that the Km for APS for APSK was ~7.5 fold, lower (i.e., higher affinity) compared to ATPS. This makes logical sense in that for ATPS domain, the product APS must diffuse with ease, to be bound fairy tightly as a substrate with APSK domain for forming the product PAPS. In addition, the cleaved PPi is immediately acted on by the ubiquitous pyrophosphatase to form 2Pi, driving the ATPS reaction forward, at same time makes the backward reaction unfavorable. Thus, the catalytic efficiency is manipulated in the PAPSS (fused gene product) by differential binding affinity. The reported phosphotransferase motif "**TLDGD**" found in APSK has been noted in many enzymes. For e.g., 3′-nucleotidases use similar motif in dephosphorylating the ribosyl-phosphate. The question of how one is a kinase, and the other is a phosphatase could in part be decided by neighboring residues? In hPAPSS1 the linear distance between Walker A/P-loop motif and phosphotransferase motif happens to be 21 residues. Similarly, the spacing between Walker A/P-loop motif and phosphotransferase motif, in hPAPSS2a is 17 and in hPAPSS2b it is 20 residues (Venkatachalam unpublished). In PAPase, (Hal2p) complexed with calcium, magnesium, and reaction substrate PAP, there are prominent residues that are about 5Å closer are Glu 72, Asp 142, Asp 145, Thr147 and Asp 294 (PDB ID: 1KA1). [23]. The linear sequence of the motif in this enzyme happens to be $D_{142}PID_{145}GT$. Various 3′-phosphate interactions are described in Ref. [24]. Future studies are underway to delineate the exact mechanism of decision forming neighboring residues/folds required for kinases versus phosphatases.

The identification of group of eukaryotic proteins involved in DNA replication initiation as putative DNA dependent ATPases; with a modified Walker A motif pattern and a common arrangement of conserved motifs for three large groups of DNA-dependent and RNA-

Table 1A
Describes the average of four values of APS formed (fmol/min/mg) in mutant D1 (D87A), D2 (D89A), (T85A), wild type (WT) and Mock. The standard error (SE) for each was also calculated.

Samples	D1 APS (fmol/min/mg)	D2 APS (fmol/min/mg)	T APS (fmol/min/mg)	Wt APS (fmol/min/mg)	Mock APS (fmol/min/mg)
1	126.3	89.5	30.3	67.8	1.19
2	174.1	69.9	36.2	43.3	3.29
3	121	202.6	82.1	82.7	3.2
4	85	101.2	50.2	87	0.36
Average	126.6	115.8	49.7	70.2	2.01
Standard Deviation	36.59	59.28	23.15	19.73	1.47
Standard Error	18.29	29.64	11.58	9.87	0.73

dependent, ATPases has been described in many organisms including small viruses [25]. Haloacid dehalogenase (HAD); superfamily of aspartate-nucleophile hydrolases (pfam 00702) contains DxDx (T/V) catalytic motif common to this superfamily [26]. This suggest that the motif DxD (T/V) present in APSK is an ancient motif well preserved and involved in phosphorylation/dephosphorylation. Many of the viruses (T antigen of SV40 (GenBank J02400), human polyoma virus (PyV; J02228), El protein of bovine papilloma virus type 1; (BPVI; ×02346); human papilloma virus type 18 (HPV18; ×05015); and human papilloma virus type 35 (HPV35); all contained motifs A-B-C [25]. In many proteins, Motif A is commonly called Walker A motif. The lysine residue along with two main chain amino (NH) groups called LRLR from the residues xxGK form a cavity/nest that chelates β-phosphate of ATP [8]. The nest residues form the binding cavity like an induced fit cavity without causing any gross conformational changes [8]. The upstream aromatic amino acid (F, W or Y) had been described to involve in π−π interaction with adenine residue of ATP [27]. The P-loop is a modified Rossman fold (β-α-β) that consists of beta sheet followed by a loop containing Motif A, followed by alpha and beta sheet (i.e., β- (loop with motif A)-α-β) [27]. Interestingly hPAPSS1, possessed P-loop with motif A, followed by quasi–Motif B and poorly defined Motif C (bolded residues) as indicated below.

"T_{53}**VWLTGLSGAGKTTVSMALEEYLVCHGIPC**Y**TLDGD**NIRQGL
NKNLGFSPEDREENVRRIAEVAKLF**A**DAGLVCITSFISPYTQDRNN
ARQIHEGASLPFFEVFVDAPLHVCEQRDVKGLYKKARAGEIKGFTG
IDSEYP"

Thus, feel the region "DGDN" in which the two aspartic residues are located must be related to the archaic motif B. In this report one could hypothesize that APSK would bind to ATP and would function like archaic ATPase to split ATP into ADP and Pi. In hPAPSS once APSK domain binds to ATP one of the D is simply stabilizing the Mg^{2+} with ATP and the other D will split the γ-phosphoryl by β-carboxylate anion base reaction. The unstable transient γ-carboxyl-P will then be transferred to 3′-OH of the tightly bound APS to form PAPS. Our inability to trap radioactive phospho species with D_{87} and D_{89} suggest one of the residues is critical for stabilizing the ATP binding and the other is perhaps involved in P-transfer. It is interesting hPAPSS2b traps putative carboxy-P more efficiently (Fig. 4, lane 6) relative to hPAPSS1 (Fig. 4, lane 3) a property intrinsic to the differences in catalysis type/efficiency. It is indeed fascinating that both phosphatase (splitting of ATP) and phosphorylation (addition of phosphate to 3′-OH) to form PAPS are both happening at the same active site. Crystal structure of PAPSS1 reveals dimer [28] as the native structure, where one monomer while bound to ADP the other monomer is constrained by salt bridge of APSK-[Glu74-Arg445]-ATPS [29]. This means a pendulum type motion might be happening where the catalytically active monomer would not engage in Glu74-Arg445 interaction [29]. In the next round of catalysis the salt bridged ATPS would bring ATP near the HNGH motif along with sulfate, salt bridge broken and the APS kinase poised in distance for ATPS catalysis. This would also mean APSK-APSK interaction would be slightly altered where salt bridge interaction had to be alternated. The flexible linker between ATPS-APSK must be facilitating the distancing/pendulum movement. hPAPSS1 when assayed for APSK was purpoted to show uncompetitive inhibition towards APS [30,31] leading to speculate that the APS exit from ATPS and entry into APSK domain must be timed on a nanoscale to have continuous flow of product formation. This tight regulation is perhaps needed to limit

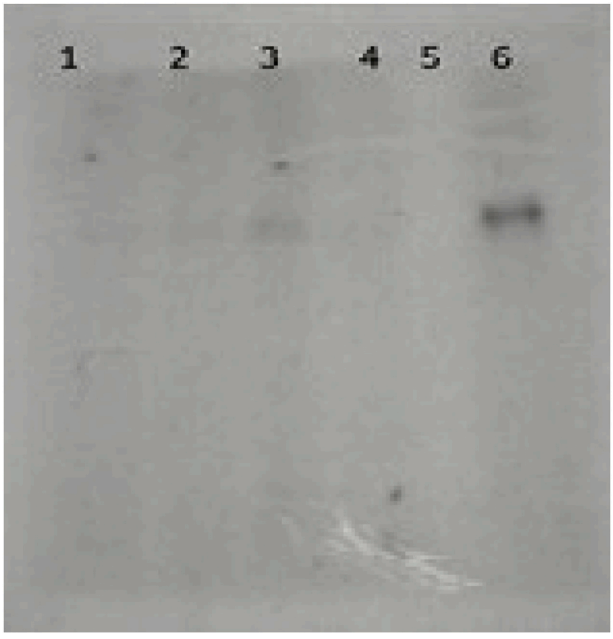

Fig. 4. Autoradiogram of SDS-PAGE of γP^{32}-ATP reacted hPAPSS (Lane 1: D1 (D87A), Lane 2: D2 (D89A) Lane 3: hPAPSS1, Lane 4: mock control (non-transformed *E. coli* extract), Lane 5: empty and Lane 6: hPAPSS2b. γP^{32}-ATP labeled samples were briefly spun and ~38 μL was loaded on to 10% SDS-PAGE gels (Novex) and electrophoresed. The gel was then dried and exposed to X-ray film overnight.

Table 1B
Same sets of samples described in Table 1A was also assessed for overall PAPS formation in the same reaction assays. Table 1B describes the PAPS formed (fmol/min/mg).

Samples	D1 PAPS (fmol/min/mg)	D2 PAPS (fmol/min/mg)	T PAPS (fmol/min/mg)	Wt PAPS (fmol/min/mg)	Mock PAPS (fmol/min/mg)
1	2.81	9.22	29.36	102.4	1.38
2	3.59	1.13	114.7	112.2	0.24
3	17.54	25.22	151.6	58.8	−0.26
4	0.84	13.6	65.3	38.8	−0.96
Average	6.195	12.2925	90.24	78.05	0.1
Standard Deviation	7.65	10.04	53.82	34.97	0.98
Standard Error	3.82	5.02	26.91	17.48	0.49

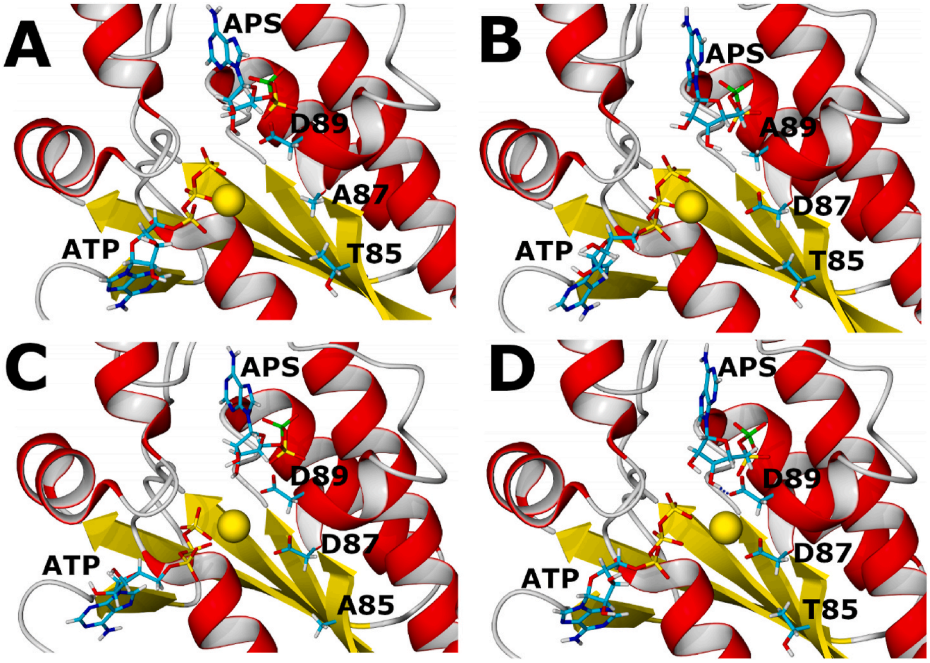

Fig. 5. Molecular Docking: APS and MgATP docked into APSK-domain. Panel A: D1 (D87A), Panel B: D2 (D89A), Panel C: T85A, Panel D: WT. The protein is shown in ribbon presentation with helices in red and beta-structure in yellow. The docked ligands are shown in an atomistic representation with corresponding colors. The Mg_2^+ ion is shown as a yellow ball. In panel D the beta-carboxyl group of D87 to Mg_2^+ distance of ~1.8 Å is represented as a blue dotted line. Interestingly the beta-carboxyl of residue D89 is close enough to gamma-P of ATP and 3′-OH of the ribose of APS poised for transient caboxy-P formation and eventual 3′-OH transfer on to APS to form 3′-OP that is PAPS. In D87A (panel A) the Mg2+ is far from alanine coordinated by beta and gamma phospate of ATP. Likewise D89A (panel B) shows the magnesium far from A89 or D87. (For interpretation of the references to color in this figure legend, the reader is referred to the Web version of this article.)

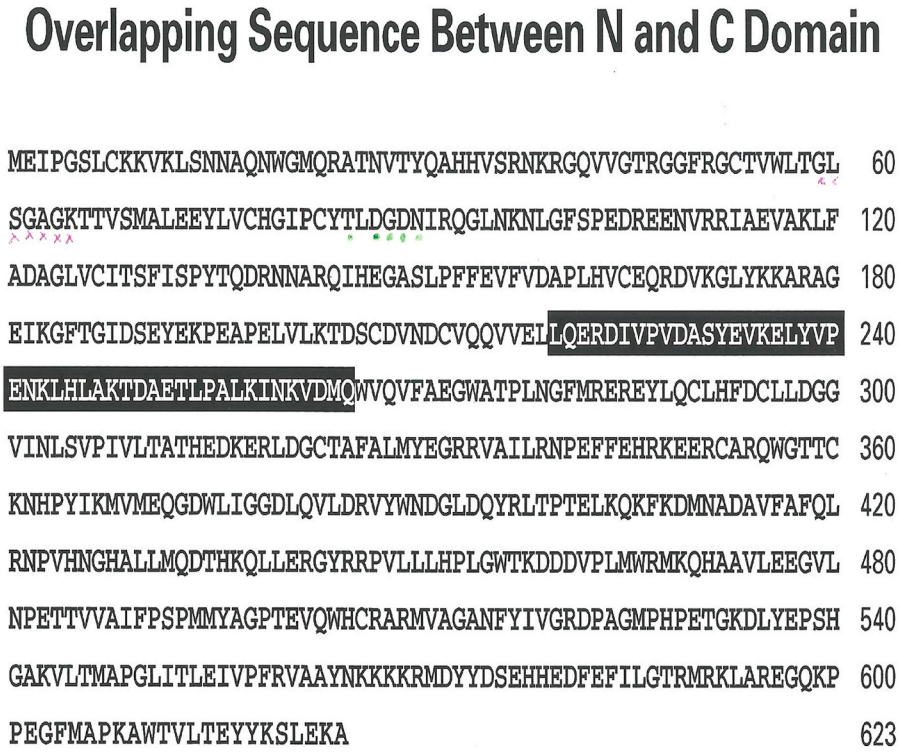

Fig. 6. Linear sequence of hPAPSS1 is depicted. Bolded region indicates the linker region required from both ATPS and APSK activities. Lack of the linker sequence abolishes both ATPS and APSK activity estabilshing the role of linker in the proper release of APS from ATPS to the APSK for PAPS formation a process that could be facilitated by crosstalk between asymmetric monomeric subunits of dimer.

/regulate the over all production of PAPS for sulfuryl tranfer reaction catalyzed by sulfotransferases (SULT's). This interaction would alter D_{87}, D_{89} residue distances poised for 3′-phosphorylation (Venkata chalam and Ettrich unpublished). Functional ATP Binding Cassette proteins appears to be a 'nucleotide-sandwich dimer with ATP flanked by the Walker A and B motifs of one ABC and the signature motif and D-loop of the other [27]. Such asymmetric catalysis and cooperation between the two monomers had been noticed in totally unrelated mammalian fatty acid synthase and functions in head to tail manner [32,33]. The mechanistic details and communication between ATPS and APSK in dimeric configuration is underway.

Thermodynamically ATPS in the forward direction in binding to ATPS and sulfate is relatively unfavorable partly due to poor ATP-Mg^{2+} chelation between α−β phosphates of ATP. Whereas in APSK the ATP

Table 2
Binding energies as given by the autodock VINA scoring function for WT and mutants. The standard deviation is calculated from all poses in a given cluster.

Compounds	D87A Binding energy [kcal/mol]	D89A Binding energy [kcal/mol]	T85A Binding energy [kcal/mol]	WT Binding energy [kcal/mol]
APS	10.9 +-1.4	10.4 +-0.6	11.0 +-1.2	10.7 +-1.6
Mg^{2+} + ATP	10.4 +-0.5	10.3 +-0.6	10.1 +-0.4	10.4 +-0.8

binding and APS binding is favored in the thermodynamic forward direction. In part this is because of ATP-Mg^{2+} chelation is very strongly facilitated by DGDN (BM motif/Walker B) [34,35] in APSK. The Mg^{2+} bidentate chelation induces minimal torsional strain/minimal change in dihedral energy or force and has no effect on the catalytic mechanism of ATP hydrolysis, whereas binding of Mg^{2+} lengthens the Pγ-Oσ bond from 1.9 to 3Å [36]. Thus, the ATP-Mg^{2+} chelation stretches the Pγ-Oσ bond making it facile for phosphorolysis [36]. Molecular docking results (Fig. 5) suggest a potential role of D87 in Mg_2^{+}-ATP chelation of hPAPSS1. The process of 3'-phosphorylation of APS could be aided by aspartic 89 [35] and mutation of the bm motif (86LDGDNhRxhh (N/S)(K/R)97) in PAPSS results in lack of PAPS formation and brachymorphism in mouse [34]. It is possible that the β-carboxylate oxy anion of D89 would first react with gamma phosphoryl of ATP by forming a transient, very unstable, carboxy-phosphate enzyme intermediate (Fig. 4 results). We propose in the second step, the 3′-OH of APS in the 3′-O^- base form, would react with D89 carboxyl-phosphate to form 3′-OP a phosphorylated APS, i.e., PAPS and a regenerated β-carboxylate/carboxyl through water splitting. This contention is supported by data from molecular docking that shows the 3'-OH within 1.8 Å to the carboxyl of D89 (Fig. 5, panel D). Further studies are underway to delineate the details of the APSK mechanism during PAPS formation. In many prenyl transferases, pyrophosphate-Mg^{2+} is stabilized by DDxxD motif and in squalene synthase two such DDxxD motif been reported to be required for PPi-Mg^{2+} binding [37]. The molecular docking of Mg^{2+}-ATP and APS into WT and single point mutant APSK domain of hPAPSS1 shows similar binding energies for both substrates (Mg^{2+}-ATP) and APS (Table 2). This indicates that T85, D87, and D89 do not contribute significantly to initial binding but the D87 and D89 probably play a major role in the actual reaction rate/mechanism as discussed above. The lack of clear DDxxD or DxxD motif would make the ATP-Mg^{2+} binding/stabilization and splitting of ATP difficult as with ATPS or easier as in APSK. The lack of metal requirement of PAPS binding in sulfotransferases (SULT's) and APS binding in ATPS clearly demostrates that sulfuryl transfer or sulfuryl anion stabilization involves different mechanism such as positively charged arginine residues [24] as opposed to Mg^{2+}involvement in APSK for organo-sulfate binding shown in this paper.

Roles

Dr. K.V. Venkatachalam: Design, conception, execution of ideas for experimental, interpretation, bioinformatics, crafting/writing and communication of the article.

Dr. R. Rudiger Ettrich: Performed the entire computational work published in this paper. Methods, results figures and discussion part corresponding to *in silico* studies are contributions from Dr. R. Ettrich.

Declaration of competing interest

The authors claim No conflicts of interest.

Acknowledgements

Experimental parts were performed by NIH summer student Rita Sneeringer. We thank students who partcipiated as assistants in learning either experimental or in silico studies as part of their higher education process.

References

[1] K.V. Venkatachalam, Human 3'-phosphoadenosine 5'-phosphosulfate (PAPS) synthase: biochemistry, molecular biology and genetic deficiency, IUBMB Life 55 (1) (2004) 1–11.
[2] K.V. Venkatachalam, H. Akita, C.A. Strott, Molecular cloning, expression, and characterization of human bifunctional 3'-phosphoadenosine 5'-phosphosulfate synthase and its functional domains, J. Biol. Chem. 273 (30) (1998) 19311–19320.
[3] K.V. Venkatachalam, H. Fuda, E.V. Koonin, C.A. Strott, Site-selected mutagenesis of a conserved nucleotide binding HXGH motif located in the ATP sulfurylase domain of human bifunctional 3'-phosphoadenosine 5'-phosphosulfate synthase, J. Biol. Chem. 274 (5) (1999) 2601–2604.
[4] J.E. Walker, M. Saraste, M.J. Runswick, N.J. Gay, Distantly related sequences in the alpha- and beta-subunits of ATP synthase, myosin, kinases and other ATP-requiring enzymes and a common nucleotide binding fold, EMBO J. 1 (8) (1982) 945–951.
[5] C. Ramakrishnan, V.S. Dani, T. Ramasarma, October, A conformational analysis of Walker motif A [GXXXXGKT(S)] in nucleotide-binding and other proteins, Protein Eng. 15 (10) (2002) 783–798.
[6] M. Saraste, P.R. Sibbald, A. Wittinghofer, November, The P-loop–a common motif in ATP- and GTP-binding proteins, Trends Biochem. Sci. 15 (11) (1990) 430–434.
[7] J.D. Watson, E.J. Milner-White, A novel main-chain anion binding site in proteins: the nest. A particular combination of phi,psi values for successive residues gives rise to anion binding sites that occur commonly and are found at functionally important regions, J. Mol. Biol. 315 (2002) 171–182.
[8] A. Bianchi, C. Giorgi, P. Ruzza, C. Toniolo, E.J. Milner-White, A synthetic peptide designed to resemble a proteinaceous P-loop nest is shown to bind inorganic phosphate, Proteins 80 (2012) 1418–1424.
[9] A.T. Deyrup, S. Krishnan, B.N. Cockburn, N.B. Schwartz, Deletion and site-directed mutagenesis of the ATP-binding motif (P-loop) in the bifunctional murine ATP-sulfurylase/adenosine 5'-phosphosulfate kinase enzyme, J. Biol. Chem. 273 (1998) 9450–9456.
[10] J.-F. Collet, V. Stroobant, M. Pirard, G. Delpierre, E.V. Schaftingen, A new class of phosphotransferases phosphorylated on an aspartate residue in an amino-terminal DXDX(T/V) motif, J. Biol. Chem. 273 (No. 23) (1998) 14107–14112.
[11] L. Aravind, E.V. Koonin, A novel family of predicted phosphoesterases includes Drosophila prune protein and bacterial RecJ exonuclease, Trends Biochem. Sci. 23 (1998) 17–19.
[12] A. Matte, H. Goldie, R.M. Sweet, L.T. Delbaere, Crystal structure of Escherichia coli phosphoenolpyruvate carboxykinase: a new structural family with the P-loop nucleoside triphosphate hydrolase fold, J. Mol. Biol. 256 (1996) 126–143.
[13] H. Fuda, C. Shimizu, Y.C. Lee, et al., Characterization and expression of human bifunctional 3'-phosphoadenosine 5'-phosphosulphate synthase isoforms, Biochem. J. 365 (Pt 2) (2002) 497–504.
[14] E.B. Lansdon, A.J. Fisher, I.H. Segel, Human 3'-phosphoadenosine 5'-phosphosulfate synthetase (isoform 1, brain): kinetic properties of the adenosine triphosphate sulfurylase and adenosine 5'-phosphosulfate kinase domains, Biochemistry 43 (14) (2004) 4356–4365.
[15] E. Krieger, G. Koraimann, G. Vriend, Increasing the precision of comparative models with YASARA NOVA-a self-parameterizing force field, Proteins Struct. Funct. Bioinf. 47 (3) (2002) 393–402.
[16] E. Krieger, G. Vriend, YASARA View—molecular graphics for all devices—from smartphones to workstations, Bioinformatics 30 (20) (2014) 2981–2982.
[17] N. Sekulic, K. Dietrich, I. Paarmann, S. Ort, M. Konrad, A. Lavie, Elucidation of the active conformation of the APS-kinase domain of human PAPS synthetase 1, J. Mol. Biol. 367 (2007) 488–500.
[18] A. Jakalian, D.B. Jack, C.I. Bayly, Fast, efficient generation of high-quality atomic charges. AM1-BCC model: II, Parameterization and validation J Comput Chem 23 (2002) 1623–1641.
[19] J. Wang, R.M. Wolf, J.W. Caldwell, P.A. Kollman, D.A. Case, Development and testing of a general amber force field, J. Comput. Chem. 25 (2004) 1157–1174.
[20] J.J.P. Stewart, MOPAC: a semiempirical molecular orbital program, J.Comp.Aided Mol.Des. 4 (2000) 1–103.
[21] A. Klamt, Conductor-like screening model for real solvents: a new approach to the quantitative calculation of solvation phenomena, J. Phys. Chem. 99 (1995) 2224–2235.
[22] O. Trott, A.J. Olson, AutoDock VINA: improving the speed and accuracy of docking with a new scoring function, efficient optimization and multithreading, J. Comput. Chem. 31 (2010) 455–461.
[23] S. Patel, M. Martinez-Ripoll, T.L. Blundell, A. Albert, Structural enzymology of Li(+)-sensitive/Mg(2+)-dependent phosphatases, J. Mol. Biol. 320 (2002) 1087–1094.
[24] K.V. Venkatachalam, Biochemical sulfuryl group transfer from 3'Phosphoadenosine 5'-phosphosulfate (PAPS) versus phosphoryl transfer from ATP: what can Be learnt? Biochem Physiol 5 (2016) 1.

[25] Koonin EV (June, A common set of conserved motifs in a vast variety of putative nucleic acid-dependent ATPases including MCM proteins involved in the initiation of eukaryotic DNA replication, Nucleic Acids Res. 21 (11) (1993) 2541–2547.
[26] M.C. Morais, W. Zhang, A.S. Baker, G. Zhang, D. Dunaway-Mariano, K.N. Allen, The crystal structure of bacillus cereus phosphonoacetaldehyde hydrolase: insight into catalysis of phosphorus bond cleavage and catalytic diversification within the HAD enzyme superfamily, Biochemistry 29 (34) (2000) 10385–10396.
[27] S.V. Ambudkar, I.W. Kim, D. Xia, Z.E. Sauna, February, The A-loop, a novel conserved aromatic acid subdomain upstream of the Walker A motif in ABC transporters, is critical for ATP binding, FEBS Lett. 580 (4) (2006) 1049–1055.
[28] S. Harjes, A. Scheidig, P. Bayer, Expression, purification and crystallization of human 3'-phosphoadenosine-5'-phosphosulfate synthetase 1, Acta Crystallogr. D 60 (Pt 2) (2004) 350–352.
[29] S. Harjes, P. Bayer, A.J. Scheidig, The crystal structure of human PAPS synthetase 1 reveals asymmetry in substrate binding, J. Mol. Biol. 347 (3) (2005) 623–635.
[30] E.B. Lansdon, A.J. Fisher, I.H. Segel, Human 3'-phosphoadenosine 5'-phosphosulfate synthetase (isoform 1, brain): kinetic properties of the adenosine triphosphate sulfurylase and adenosine 5'-phosphosulfate kinase domains, Biochemistry 43 (14) (2004) 4356–4365.
[31] N. Sekulic, M. Konrad, A. Lavie, Structural mechanism for substrate inhibition of the adenosine 5'-phosphosulfate kinase domain of human 3'-phosphoadenosine 5'-phosphosulfate synthetase 1 and its ramifications for enzyme regulation, J. Biol. Chem. 282 (30) (2007) 22112–22121.
[32] S. Smith, A. Witkowski, A.K. Joshi, July, Structural and functional organization of the animal fatty acid synthase, Prog. Lipid Res. 42 (4) (2003) 289–317.
[33] S.J. Wakil, Fatty acid synthase, a proficient multifunctional enzyme, Biochemistry 28 (11) (1989) 4523–4530.
[34] B. Singh, N.B. Schwartz, Identification and functional characterization of the novel BM-motif in the murine phosphoadenosine phosphosulfate (PAPS) synthetase, J. Biol. Chem. 278 (2003) 71–75.
[35] Nikolina Sekulic, Kristen Dietrich, Ingo Paarmann, Stephan Ort, Manfred Konrad, Arnon Lavie, Elucidation of the active conformation of the APS kinase domain of human PAPS synthetase 1, J. Mol. Biol. 367 (2) (2007) 488–500.
[36] Christopher B. Harrison, Klaus Schulten, Quantum and classical dynamics simulations of ATP hydrolysis in solution, J. Chem. Theor. Comput. 8 (7) (2012) 2328–2335.
[37] Jayvardhan Pandit, Dennis E. Danley, Gayle K. Schulte, Stacy Mazzalupo, Thomas A. Pauly, Cheryl M. Haywardi, Ernest S. Hamanakai, John F. Thompsoni, H. James Harwood Jr., Crystal structure of human squalene synthase, J. Biol. Chem. 275 (39) (2000) 30610–30617.